NONLINEAR ANALYSIS FOR AXISYMMETRIC ELASTIC STRESSES IN RING-STIFFENED, SEGMENTED SHELLS OF REVOLUTION

David Bushnell

Lockheed Missiles and Space Company
Palo Alto, California

September 1968

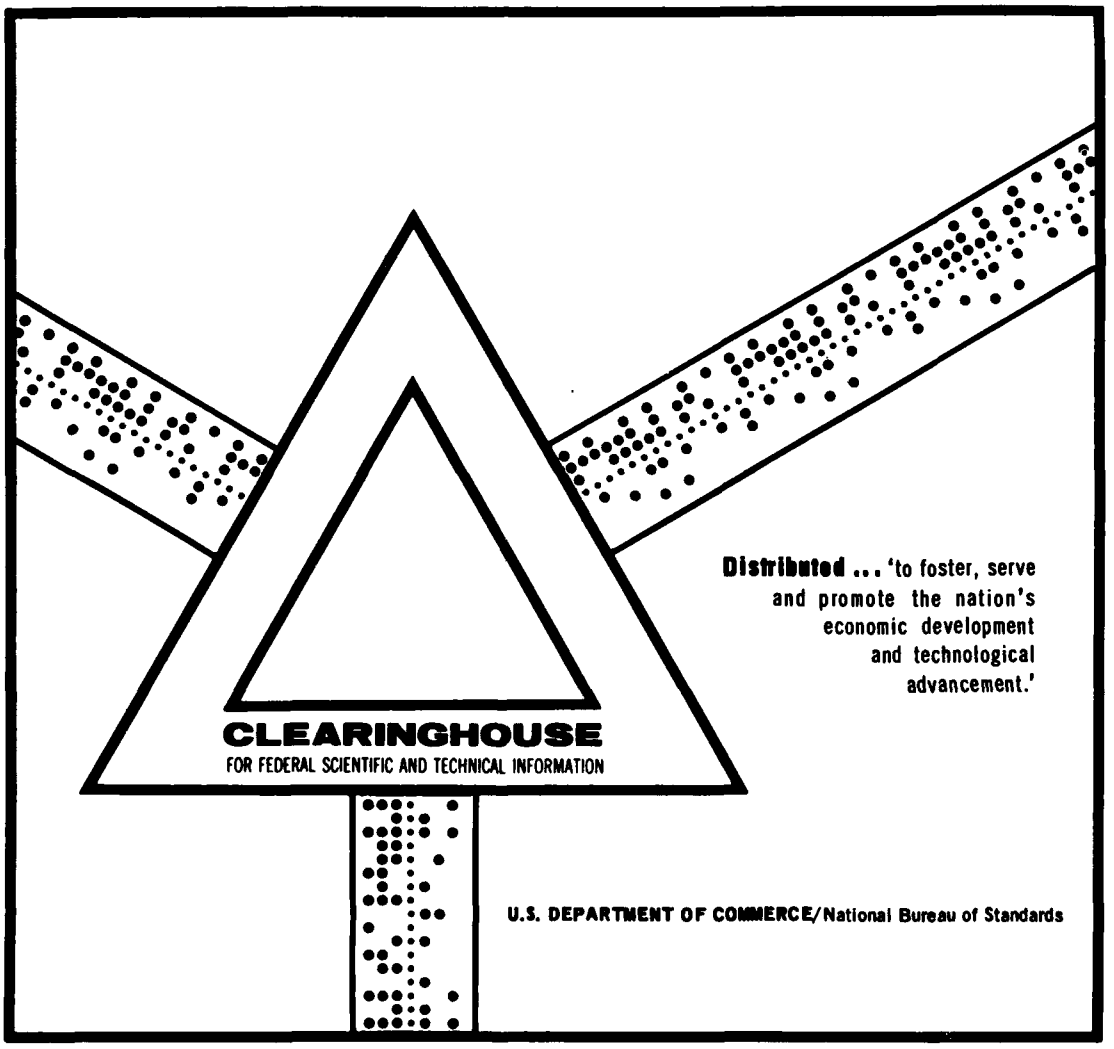

DISCLAIMER NOTICE

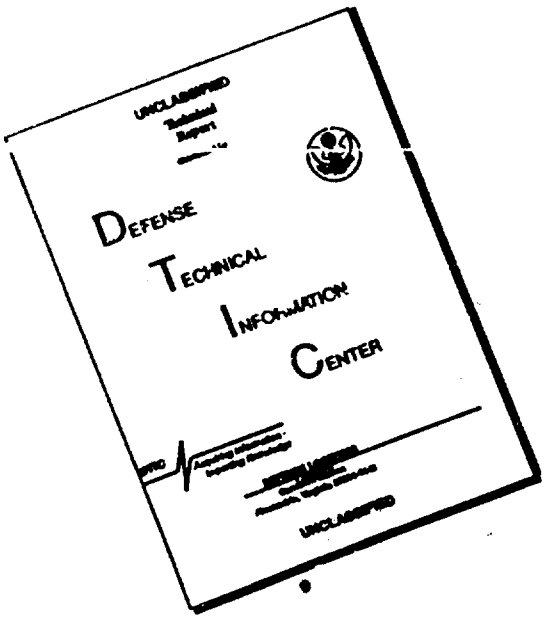

THIS DOCUMENT IS BEST QUALITY AVAILABLE. THE COPY FURNISHED TO DTIC CONTAINED A SIGNIFICANT NUMBER OF PAGES WHICH DO NOT REPRODUCE LEGIBLY.

NONLINEAR ANALYSIS FOR AXISYMMETRIC ELASTIC STRESSES IN RING-STIFFENED, SEGMENTED SHELLS OF REVOLUTION

by

DAVID BUSHNELL

This research was sponsored by the Structural Mechanics Laboratory of the Naval Ship Research and Development Center under Naval Ship Systems Command Subproject SF 013 03 02, Task 1952.

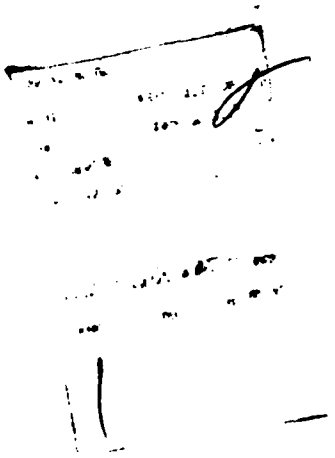

NONLINEAR ANALYSIS FOR AXISYMMETRIC ELASTIC STRESSES IN RING-STIFFENED, SEGMENTED SHELLS OF REVOLUTION

by
David Bushnell

N-26-68-2 September 1968

This research was sponsored by the Structural Mechanics Laboratory of the Naval Ship Research and Development Center under Naval Ship Systems Command Subproject SF 013 03 02, Task 1952.

Lockheed Palo Alto Research Laboratory
Lockheed Missiles & Space Company
A Group Division of Lockheed Aircraft Corporation
Palo Alto, California

ABSTRACT

The finite-difference method is used for the nonlinear analysis of shells of revolution consisting of elastic shell segments of various geometries and wall constructions joined by elastic rings. The analysis and associated digital computer program were developed in response to the need for a better design tool for practical shell structures. Numerical results are presented for displacement and stress distributions in various pressure vessels. Particular emphasis is given to systems in which nonlinear effects are important and may influence the design. Values calculated with linear theory are compared with those from nonlinear theory.

Introduction

The work described herein represents part of an effort to develop a user-oriented computer program for the analysis of the stress, stability, and vibration of elastic, ring-stiffened, segmented shells of revolution with various wall constructions and submitted to various axisymmetric load systems.

Such a structure is shown in Fig. 1, for example. This shell consists of four segments, labeled ① , ② , ③ , and ④ . Segment ① is a meridionally stiffened coverplate or hatch; ② is a spherical segment reinforced by T-shaped rings; ③ is a cylinder with ring stiffeners; and ④ is an ellipsoidal closure of variable thickness. The thickness of all of the segments varies near the junctures. While Fig. 1 does not represent an actual design, it does illustrate some of the features incorporated into the design of practical shell structures. The shell structure may be loaded by internal or external pressure, and line loads and moments may be applied to any or all of the ring reinforcements. The designer may be interested in the behavior of such a composite shell structure with respect to stress, stability, and vibration.

A user-oriented computer program called BOSOR 2 has been written for the general analysis of shells of the type shown in Fig. 1. This program is a "next generation" successor to the code BOSOR described in Refs. 1 and 2. The program BOSOR 2 consists of two parts: a part in which the axisymmetric stresses and displacements are calculated from nonlinear theory, and a part in which nonsymmetric loads and vibration frequencies are calculated from a linear eigenvalue analysis. The linear stability and vibration analyses with numerical results are given in Ref. 3.

In this paper the nonlinear analysis for axisymmetric stresses and displacements is described, and numerical results are given for examples in which nonlinear effects are significant.

The method of finite-differences is used to calculate axisymmetric stress states in segmented, ring-stiffened, elastic shells of revolution with various types of wall construction. Nonlinear equations similar to those developed by Reissner (Ref. 4) are used in the analysis. The work is an extension of that presented in Ref. 5. The applicability of the analysis of Ref. 5 is extended to include:

1. Analysis of segmented (composite) shells, such as cylinder-cone combinations or joined shells with dissimilar wall characteristics.
2. Analysis of shells with discrete rings at a number of stations along the meridian and at the boundaries.
3. Analysis of shells, the wall properties of which vary in the meridional direction.
4. Increased generality of the type of axisymmetric loading applied to the shell.

In addition, much effort has been devoted to making the computer program user-oriented. It is felt that the main contribution of this paper to the art of shell analysis is the development of a design tool for practical shell structures with ring supports, in which nonlinear effects may be important. In this respect the paper represents extensions to the work of Kalnins (Ref. 6), Radkowski, et al (Ref. 7), Mason, et al (Ref. 8), Wilson and Spier (Ref. 9), and Sepetoski, et al (Ref. 10).

One of the more important extensions of the analysis of Ref. 5 is the addition of a capability to treat segmented shells. This capability can also be used to advantage for simple shells. For instance a rather long cylinder submitted to pressure loading can be divided artificially into three segments: two edge segments in which stresses and displacements vary rapidly over short lengths, and a central segment in which deformations are uniform. The station spacing in the finite difference mesh can be small in the two edge segments and large in the central segment. It has been found from experience that it is better to divide the shell into segments, and thus to maintain uniform station spacing within each segment rather than to vary the station spacing within any segment. Examples are given in the section on Numerical Results in which single shells are treated in segments.

Nomenclature

A	ring cross-section area
A_{11}, A_{12}, etc.	coefficients of constitutive equations (6)
E	Young's modulus
e	ring shear center eccentricity, see Fig. 3
$\bar{H}$	radial load applied to ring, see Fig. 3
H	shell radial load, see Fig. 2
I_x, I_y, I_{xy}	moments of inertia about x, y axes; product of inertia (see Fig. 3)
i	mesh points
K	Gaussian curvature $1/R_1R_2$; also total number of mesh points
$\bar{M}$	couple applied to ring, see Fig. 3
M	shell moment/length, see Fig. 2

N	stress resultants, see Fig. 2
p	pressure, see Fig. 2
r	parallel circle radius, see Fig. 2
R	Radius of curvature
u	radial deflection, see Fig. 2
V	axial load/length in shell, see Fig. 2
$\bar{V}$	axial load/length applied to ring, see Fig. 3
β	meridional rotation, see Fig. 3
ϵ	reference surface strain
κ	reference surface change of curvature
φ	angle from horizontal to tangent to deformed meridian, see Fig. 2
ψ	stress function $\psi = rH$

Subscripts and Superscripts

$( )^n$	n^{th} iteration
$( )^+$	after meridional discontinuity, see Fig. 3
$( )^-$	before meridional discontinuity, see Fig. 3
$( )_s$	shear center of ring; also "shell"
$( )_r$	pertaining to ring
$( )'$	derivative with respect to arc length
$( )_v$	pertaining to axial (vertical)
$( )_H$	pertaining to radial (horizontal)
$( )_1$	meridional
$( )_2$	circumferential
$( )_o$	undeformed

Basic Equations

The nonlinear equations of equilibrium of a shell of revolution subjected to axisymmetric loading are presented in Ref. 4. They are:

$$(rV)' + rp_V = 0 \qquad \psi' - N_2 + rp_H = 0$$
$$(rM_1)' - \cos\varphi M_2 + \psi \sin\varphi - rV\cos\varphi = 0 \tag{1}$$

where the sign conventions are shown in Fig. 2. Here $\psi = rH$ and superscript prime indicates differentiation with respect to arc length s. The strain-displacement and curvature-displacement relations given in Ref. 4 are:

$$\epsilon_1 = \frac{\cos\varphi_o}{\cos\varphi}\left(1 + \frac{u'}{r'}\right) - 1 \qquad \epsilon_2 = u/r$$
$$\kappa_1 = \varphi_o' - \varphi' \qquad \kappa_2 = (\sin\varphi_o - \sin\varphi)/r \tag{2}$$

and the compatibility equation derived by elimination of u from Eqs. (2a) and (2b) is

$$\cos\varphi_o(r\epsilon_2)' - \cos\varphi r'\epsilon_1 = r'(\cos\varphi - \cos\varphi_o) \tag{3}$$

The basic equations are the compatibility Eq. (3) and the third equilibrium Eq. (1c). The basic dependent variables are φ and ψ. The strains and their derivatives are assumed small compared to unity. With $r' = \cos\varphi_o$ Eqs. (1c) and (3) can be written in the form

$$(rX_1)' - \cos\varphi X_2 = f \tag{4}$$

where in Eq. (1c): in Eq. (3)

$$X_1 = M_1 \qquad X_1 = \epsilon_2$$
$$X_2 = M_2 \qquad X_2 = \epsilon_1 \tag{5}$$
$$f = rV\cos\varphi - \psi\sin\varphi \qquad f = \cos\varphi - \cos\varphi_o$$

The constitutive equations for orthotropic shells can be written in the form

$$\begin{Bmatrix} \epsilon_1 \\ \epsilon_2 \\ M_1 \\ M_2 \end{Bmatrix} = \begin{bmatrix} A_{11} & A_{12} & A_{13} & A_{14} \\ A_{21} & A_{22} & A_{23} & A_{24} \\ A_{31} & A_{32} & A_{33} & A_{34} \\ A_{41} & A_{42} & A_{43} & A_{44} \end{bmatrix} \begin{Bmatrix} N_1 \\ N_2 \\ \kappa_1 \\ \kappa_2 \end{Bmatrix} \tag{6}$$

Reissner (Ref. 4) formulated the equilibrium and compatibility equations for the case of moderate rotations by assuming that

$$\cos\varphi = \cos(\varphi_o - \beta) \approx \left(1 - \tfrac{1}{2}\beta^2\right)r' + \beta r/R_2$$
$$\sin\varphi = \sin(\varphi_o - \beta) \approx \left(1 - \tfrac{1}{2}\beta^2\right)r/R_2 - \beta r' \tag{7}$$

The dependent variables of the nonlinear stress analysis are now β and ψ. Since the equilibrium and compatibility equations (4) are written in terms of ϵ_1, ϵ_2, M_1, and M_2, which through Eqs. (6) are expressed in terms of N_1, N_2, κ_1, and κ_2, one must obtain the latter quantities in terms of β and ψ, thus:

$$rN_1 = \psi\cos\varphi + rV\sin\varphi$$
$$N_2 = \psi' + rp_H$$
$$\kappa_1 = \beta' \tag{8}$$
$$\kappa_2 = \left(\beta r' + \tfrac{1}{2}\beta^2 r/R_2\right)/r$$

Substitution of the right-hand-sides of Eqs. (8) in Eqs. (6) and of Eqs. (6c, d) in the left-hand-side of Eq. (4) and use of Eqs. (7) for $\cos\varphi$ and $\sin\varphi$, leads to:

$$rA_{32}\psi'' + [r'(A_{31} - A_{42} + A_{32}) + rA'_{32}]\psi' + [r'A'_{31} - r'^2A_{41}/r - A_{31}rK]\psi + rA_{33}\beta''$$
$$+ [r'(A_{33} + A_{34} - A_{43} - rVA_{31}) + rA'_{33}]\beta' + [r'A'_{34} - r'^2A_{44}/r - A_{34}rK$$
$$+ rV(A_{31}rK - r'A'_{31} + r'^2A_{41}/r - A_{41}r/R_2^2) + A_{31}rr'\,p_v - A_{42}r^2p_H/R_2]\beta$$
$$+ (A_{31} - A_{42})(r/R_2)\psi'\beta + (A_{31}r'/R_1 + rA'_{31}/R_2 - 2r'A_{41}/R_2)\psi\beta + (rA_{31}/R_2)\psi\beta'$$
$$- (A_{43} - A_{34})(r/R_2)\beta\beta' - \tfrac{1}{2}(3A_{44}r'/R_2 - A_{34}r'/R_1 - A'_{34}r/R_2)\beta^2$$
$$+ rV(A_{31}r'/R_1 + A'_{31}r/R_2 - A_{41}r'/R_2) + A_{32}(r^2p_H)' + r^2p_H(A'_{32} - r'A_{42}/r)$$
$$- A_{31}r^2p_v/R_2 \qquad (9)$$

The expression (9) represents the left-hand-side of the equilibrium Eq. (4). The left-hand-side of the compatibility equation is obtained from Eq. (9) by the replacement of A_{3i} by A_{2i} and A_{4i} by A_{1i}. This substitution is possible because ϵ_2 in the compatibility equation plays the same role as M_1 in the equilibrium equation and ϵ_1 plays the same role as M_2. The terms not involving A_{ij}, denoted f in Eq. (4) are given in Eqs. (5). In the development of Eq. (9) terms of higher order than quadratic in the dependent variables have been dropped. Also, terms involving the product of a load and β^2 have been dropped.

Boundary Conditions and Compatibility Conditions

Figure 3 shows a portion of a shell meridian with a discontinuity B-A. There may be a ring associated with this discontinuity. The shear center of the ring is

located at point C. External forces and moment $\bar{V}$, $\bar{H}$, and $\bar{M}$ are applied to the ring axis of shear centers. The shell ends A and B also exert forces and moments V_s, H_s, and M_s on the ring, those at A denoted by a superscript plus and those at B by a superscript minus. There are five compatibility conditions which must be satisfied at the discontinuity: compatibility of the two force components and the moment, and compatibility of the meridional rotation β and horizontal displacement u_{Hr}.

If the ring centroid coincides with the shear center, the horizontal force compatibility equation is

$$B_{11}u_{Hr} + B_{12}r_s\beta = -\psi^-/r_s + \psi^+/r_s + \bar{H} \tag{10}$$

and the moment compatibility equation is

$$\begin{aligned} B_{12}u_{Hr} + B_{22}r_s\beta = {} & -r^-M_s^-/r_s^2 + r^+M_s^+/r_s^2 + \bar{M}/r_s - (rV_s)^-(e_1^- + \beta e_2^-)/r_s^2 \\ & + (rV_s)^+(e_1^+ + \beta e_2^+)/r_s^2 + \psi^-(e_2^- - \beta e_1^-)/r_s^2 \\ & + \psi^+(e_2^+ - \beta e_1^+)/r_s^2 \end{aligned} \tag{11}$$

Vertical force compatibility is represented simply by

$$(rV_s)^+ = (rV_s)^- + r_s\bar{V} \tag{12}$$

Compatibility of meridional rotation and horizontal displacement are represented by the following equations:

$$u_{Hr} = u_H^- + \beta^- e_2^- = u_H^+ + \beta^+ e_2^+ \tag{13}$$

$$\beta^+ = \beta^- \tag{14}$$

The quantities B_{11}, B_{12}, and B_{22} in Eqs. (10) and (11) are given by

$$B_{11} = EA/r_s^2 + EI_y/r_s^4 - \bar{H}/r_s$$

$$B_{12} = - EI_{xy}/r_s^4 \tag{15}$$

$$B_{22} = EI_x/r_s^4 + \frac{I_x}{Ar_s^3}\{\psi^-/r_s - \psi^+/r_s - \bar{H}\}$$

where E, A, I_x, and I_{xy} are the modulus, cross-section area, and moments of inertia of the ring about axes through the shear center (see Fig. 3.) It is clear that Eqs. (10) through (15) can be specialized for the cases where the "discontinuity" (ring) occurs at either end of the shell. The displacement continuity conditions Eqs. (13) and (14) no longer apply in these cases, and the appropriate shell forces [either $(\,)^+$ or $(\,)^-$] are set equal to zero, depending on which end of the shell is being considered.

The statement of the nonlinear boundary value problem is now complete. The governing equations have the form of Eq. (4), and the boundary conditions (and compatibility conditions) are given by Eqs. (10) through (14).

Solution of the Equations

All of the equations, including the boundary conditions, can be written in the form:

$$C_1\psi'' + C_2\psi' + C_3\psi + C_4\beta'' + C_5\beta' + C_6\beta + C_7\psi'\beta + C_8\psi\beta + C_9\psi\beta' + C_{10}\beta\beta' + C_{11}\beta^2 + C_{12} = 0 \tag{16}$$

The method of finite differences is used in the solution of the equations. Variable station spacing is allowed for in the analysis, but is not included in the computer program. Three-point finite difference formulas are used:

$$\psi_i' = c_1\psi_{i+1} + c_2\psi_i + c_3\psi_{i-1}$$
$$\psi_i'' = c_4\psi_{i+1} + c_5\psi_i + c_6\psi_{i-1} \tag{17}$$

where

$$c_1 = h_i/[h_{i+1}(h_i + h_{i+1})] \qquad c_4 = 2/[h_{i+1}(h_i + h_{i+1})]$$
$$c_2 = 1/h_i - 1/h_{i+1} \qquad c_5 = -2/h_i h_{i+1} \tag{18}$$
$$c_3 = -h_{i+1}/[h_i(h_i + h_{i+1})] \qquad c_6 = 2/[h_i(h_i + h_{i+1})]$$

and h_i, h_{i+1} are the meridional intervals on either side of the i^{th} mesh point. The quantities β' and β'' are given by formulas analogous to Eq. (17). Eq. (16) in finite-difference form is

$$A_{1i}\psi_{1-1} + A_{2i}\beta_{i-1} + A_{3i}\psi_i + A_{4i}\beta_i + A_{5i}\psi_{i+1} + A_{6i}\beta_{i+1} + \sum_{j=1}^{3}\sum_{k=1}^{3} B^i_{jk}\psi_{i-2+j}\beta_{i-2+k}$$
$$+ \sum_{j=1}^{3} B^i_j\beta_i\beta_{i-2+j} = F_i \qquad i = 1, 2, \ldots K \tag{19}$$

The index i denotes mesh point number and K denotes the total number of mesh points in the domain. There are two unknowns (ψ_i and β_i) for each mesh point and two equations (equilibrium and compatibility) for each mesh point [see Fig. 4(a)]. In addition, fictitious mesh points are introduced at either end of the meridian and at meridional discontinuities in order that first derivatives of ψ and β can be specified at the end points of the segment [see Fig. 4(b)]. Equations corresponding to these points are the boundary conditions or matching conditions. Hence, there is a set of $2K + 4(d + 1)$ nonlinear simultaneous algebraic equations, where d is the number of meridional discontinuities.

These equations are solved by use of the Newton-Raphson method. Thurston (Ref. 11) has discussed this method as applied to various nonlinear problems involving many degrees of freedom. As applied in this case, the Newton-Raphson procedure is as follows: Eqs. (19) are linearized through substitution of

$$\psi_i^{n+1} = \psi_i^n + \Delta\psi_i \quad , \quad \beta_i^{n+1} = \beta_i^n + \Delta\beta_i \tag{20}$$

where n refers to "iteration number" and $\Delta\psi_i$ and $\Delta\beta_i$ are correction addends for the current iteration. Equation (19) is written with $\Delta\psi_i$ and $\Delta\beta_i$ considered as the unknowns and with terms involving only ψ_i^n and β_i^n removed to the right-hand-side. Quadratic terms in $\Delta\psi_i$ and $\Delta\beta_i$ are dropped. The typical equation for the current iteration now appears as follows:

$$\begin{aligned} A^*_{1i}\Delta\psi_{i-1} + A^*_{2i}\Delta\beta_{i-1} + A^*_{3i}\Delta\psi_i + A^*_{4i}\Delta\beta_i + A^*_{5i}\Delta\psi_{i+1} + A^*_{6i}\Delta\beta_{i+1} \\ = F_i - A_{1i}\psi^n_{i-1} - A_{2i}\beta^n_{i-1} - A_{3i}\psi^n_i - A_{4i}\beta^n_i - A_{5i}\psi^n_{i+1} - A_{6i}\beta^n_{i+1} \\ - \sum_{j=1}^{3}\sum_{i=1}^{3} B^i_{jk}\psi^n_{i-2+j}\beta^n_{i-2+k} - \sum_{j=1}^{3} B^i_j\beta^n_i\beta^n_{i-2+j} \end{aligned} \tag{21}$$

The A^*_{mi}, $m = 1, 6$ contain ψ_i^n and β_i^n from the previous iteration. The terms on the right-hand-side of Eq. (21) are all known. The simultaneous linear set is solved for the vector of correction addends $\Delta\psi_i$ and $\Delta\beta_i$, and these are added to the ψ_i^n and β_i^n to give ψ_i^{n+1} and β_i^{n+1}. Iterations continue until satisfactory convergence has been obtained.

In the Newton-Raphson method a starting vector ψ_i^o, β_i^o must be assigned. If this vector is zero, the solution for the correction addends, and hence for ψ_i^1, β_i^1 is the solution of the linearized equations. Problems that are essentially nonlinear, such as that of a spherical shell submitted to a point load at the apex, are solved in the following way: Calculations begin for a small value of the load, for which the linear theory is reasonably accurate. Previous solutions ψ_i^n, β_i^n are then used as starting vectors for each new value of the load.

In order that the linear system represented by Eq. (21) be solved with a reasonable amount of computer time, one must arrange the equations so that the matrix of coefficients is strongly banded about the main diagonal. If alternate equations are equilibrium and compatibility equations and if alternate dependent variables are $\Delta\psi_i$ and $\Delta\beta_i$, the matrix shown schematically in Fig. 4(a) will result. This matrix corresponds to a shell with one meridional discontinuity. The meridian with mesh points is shown in Fig. 4(b). Each mesh point "generates" two columns and two rows in the coefficient matrix. The matching conditions labeled "Horizontal Force Compatibility," etc. are given by Eqs. (10), (11), (13) and (14), respectively. All elements not enclosed in a box are zero.

Numerical Results

Numerous test cases have been run to check the portion of the computer program BOSOR 2 which calculates the axisymmetric state of stress. The number of mesh points was varied to ensure convergence. For the test cases the stresses converge to within a few percent of the exact values with less than 100 mesh points. Two to four iterations are usually required for convergence to the solution of the governing nonlinear equations. Figures 5a and 5b show the results of one such test case. A shell of the geometry shown in Fig. 5a was analyzed by Stricklin, et al (Ref. 12), who used the matrix displacement method in a nonlinear analysis. In this application of BOSOR 2, 95 mesh points were used. Three iterations of the Newton-Raphson procedure were required before successive solutions were within 0.1% of each other. The total computer time for execution was 3.15 seconds on the Univac 1108.

Figures 6a and 6b show the meridional bending moments generated in pressurized steel hemisphere with a mismatch. Moments resulting from internal pressures of 100 psi and 10,000 psi are given in Fig. 6a. The effect of internal pressure on the moment distribution is to shorten the "decay length" of the discontinuity stress. This is in agreement with results obtained by other investigators. Figure 6b shows that external pressure has the opposite effect: the discontinuity stress "boundary layer" is increased in length due to the pressure. While the nonlinear effect of pressure on the distribution of discontinuity stresses is well known to many specialists in shell theory, it is rarely if ever accounted for in the design of shell structures. This effect could be important, for example, in the selection of positions of welds in composite shell structures.

During the manufacture of shell structures certain unplanned variations in geometry are likely to occur. Figure 7a shows an example in which the geometry near the viewport of a pressure hull for a deep submersible vehicle changed during assembly due to the weld on the meridian. The portion of the hull in the neighborhood of the apex moved inward slightly as shown by the dotted lines. The measured sinkage is shown in Fig. 7b. A curve-fitting program (Ref. 13) was applied to the measurements to calculate the variation in meridional curvature which is shown in Fig. 7c. Two curves are given in Fig. 7c, one which corresponds to curvatures calculated with 12 input points chosen from Fig. 7b and one which corresponds to curvatures calculated with 36 input points chosen from Fig. 7b. The nominal curvature is also shown in Fig. 7c. The structure shown in Fig. 7a was analyzed on the computer as a shell of two segments: the segment nearest the apex being an "out-of-round" spherical shell of variable thickness, and the other segment being a perfect spherical segment of nominal curvature and constant thickness extending to $\alpha = 90$ deg. The thickness distribution is taken from Ref. 14, and the edge of the shell at the viewport is assumed to be free. The meridional bending moments for three cases are shown in Fig. 7d. In all cases the shell is submitted to uniform external pressure of 1.0 psi. The bending moment distribution for the perfect shell agrees with that calculated in Ref. 14. This moment distribution is compared with moments for the imperfect shell in which 12 and 36 input points are used for calculation of the geometry of the variable thickness segment. Two interesting observations might be made with regard to the results: the stress distribution is rather drastically affected by the weld sinkage (the maximum stress, which occurs near the weld at the outer fiber being increased by almost a factor of two; and the moment distributions corresponding to the two different

geometrics (Fig. 7c) calculated by the curve-fitting routine are very similar, even though the input meridional curvatures are very dissimilar. Apparently, the shell behavior is related to a "smoothed" or averaged meridional curvature distribution, rather than to the rapidly changing variation of curvature shown in Fig. 7c as a dotted line. The probable explanation is that the arc length over which the rapid curvature changes occur is small compared to the attenuation length or "boundary layer" length of the discontinuity stresses for this particular shell.

Figure 8 gives the hoop stress resultants for pressurized shallow spherical shells with edge rings located as shown. Edge moments are also applied as shown. The vertical reaction coincides with the ring centroid, which is located distances e_1 and e_2 from the edge of the shell. The pressures are 0.619 psi and 0.357 psi for the two cases. It is seen that small differences in the geometry of the structure cause large differences in the stress distributions. The ring eccentricities must be accounted for in the analysis of such shell structures. As an aid to the designer the computer program can be used to find the most favorable location of the edge ring.

Figure 9 shows the maximum meridional stress in the outer fiber of an internally pressurized aluminum cryogenic tank. The geometry is shown at the top and bottom of the figure. The inner surface from the centerline to the point D is an ellipsoid and from D to the plane of symmetry is a cylinder. The thickness varies linearly between the stations where it is called out. The large increase in thickness near the juncture of the cylinder and the ellipsoid was included in the design in order to compensate for the weakening effect of a weld there. The outer fiber meridional stress is maximum at point C. As seen from Fig. 9 linear theory yields 93 ksi for

this maximum, and nonlinear theory yields 74 ksi. The results for linear theory are in good agreement with a solution obtained through use of a computer program written by Kalnins (Ref. 6).

Figure 10 shows SC4020 computer plots of stress resultants for the cryogenic tank. The plot routine was written by Dyche (Ref. 15). Various configurations were analyzed. Figures 10b and 10e correspond to a tank in which the reference surface is an ellipsoid joined to a cylinder with the thickness distributed equally on both sides of the reference surface. Figures 10a, c, d, f, and g correspond to a tank in which the same reference surface geometry is considered to be the inner surface of the shell. As seen from a comparison of Figs. 10e and 10f, the large bending stress at point C in Fig. 9 disappears if the shell is manufactured such that the reference surface is the middle surface.

Figures 10d and 10g correspond to 1/1000 of the design pressure $p = 70.3$ psi, and thus approximate the linear solution. Note that the hoop stress resultant calculated from linear theory is negative in a small region, giving an erroneous indication of the possibility of buckling at some higher pressure. Also, the hoop stress resultant at the plane of symmetry would be over-estimated by about 25% if linear theory were used for calculation of stresses at the design pressure. The bending stresses predicted by the linear theory are about twice those predicted by the nonlinear theory.

Figure 11a shows a portion of a spherical shell with a local area in which the radius of curvature is greater than the nominal radius. This "flat" area represents an imperfection in the shell, which is submitted to uniform external pressure. Figures 11b and 11c give the state of the shell just before it collapses in an axisymmetric mode. Collapse loads are calculated as described in Ref. 2.

In the plots the origin corresponds to the apex of the shell. The shell is treated as if consisting of three segments: the "flat" spot, a region approximately one "boundary layer" in length adjacent to the flat spot, and the remainder of the shell. The meridional station which corresponds to the edge of the "flat" spot is indicated by heavy vertical lines in Figs. 11b and 11c. The dotted lines in the plots of UH and UV represent the membrane solution extrapolated to the apex of the shell. The plots correspond to a load within 0.1% of the collapse load, which is 28.7% of the classical buckling load for a complete sphere of the nominal radius. In Ref. 16, a collapse load of 28.0% of the classical buckling load was found in an analysis in which the entire shell was treated as one segment. It is seen that the maximum inward displacement (UV at the apex = 0.85) is considerably greater than the maximum value of 0.7 shown in Fig. 2 of Ref. 16. Near the collapse load the displacement increases rapidly with small increments in the pressure. This case is included to illustrate the advantage of analyzing a single shell structure in segments. The input data is simpler, and fewer mesh points are required for convergence to within a prescribed error.

REFERENCES

1. Bushnell, D., Almroth, B. O., and Sobel, L. H., "Buckling of Shells of Revolution With Various Wall Constructions," Vol. 3, "User's Manual for BOSOR," NASA CR-1051, May 1968

2. Almroth, B. O. and Bushnell, D., "Computer Analysis of Various Shells of Revolution," presented AIAA 6th Aerospace Sciences Meeting, New York, Jan 1968. To appear AIAA J.

3. Bushnell, D., "Buckling and Vibration of Ring-Stiffened, Segmented Shells of Revolution," LMSC 6-78-68-37, Aug 1968

4. Reissner, E., "On Axisymmetrical Deformation of Thin Shells of Revolution," Proc. of Symposia in Applied Mathematics, Vol. III (McGraw-Hill, 1950), pp. 27–52

5. Bushnell, D., Almroth, B. O., and Sobel, L. H., "Buckling of Shells of Revolution With Various Wall Constructions," Vol. 2, "Basic Equations and Method of Solution," NASA CR 1050, May 1968

6. Kalnins, A., "Analysis of Shells of Revolution Subjected to Symmetrical and Nonsymmetrical Loads," Jl. of Appl. Mech., Vol. 31, No. 3, Sep 1964, pp. 467–476

7. Radkowski, P. P., Davis, R. M., and Bolduc, M. R., "Numerical Analysis of Equations of Thin Shells of Revolution," ARS Journal, Vol. 32, No. 1, Jan 1962, pp. 36–41

8. Mason, P., Rung, R., Rosenbaum, J., and Ebrus, R., "Nonlinear Numerical Analysis of Axisymmetrically Loaded Arbitrary Shells of Revolution," AIAA Journal, Vol. 3, No. 7, Jul 1965, pp. 1307-1313

9. Wilson, P. E. and Spier, E. E., "Numerical Analysis of Large Axisymmetric Deformations of Thin Spherical Shells," AIAA Journal, Vol. 3, No. 9, Sep 1967, pp. 1716-1725

10. Sepetoski, W. K., Pearson, C. E., Dingwell, I. W., and Adkins, A. W., "A Digital Computer Program for the General Axially Symmetric Thin Shell Problem," J. App. Mech., Dec 1962, pp. 655-661

11. Thurston, G. A., "Newton's Method Applied to Problems in Nonlinear Mechanics," J. Appl. Mech., Vol. 32, (1965) pp. 383-388

12. Stricklin, J. A., Haisler, W. E., MacDougall, H. R., and Stebbins, F. J., "Nonlinear Analysis of Shells of Revolution by the Matrix Displacement Method," presented at AIAA 6th Aerospace Sciences Meeting, New York, Jan 1968, AIAA Paper No. 68-177

13. Pennington, R. H., Introductory Numerical Analysis and Computer Methods (MacMillan, New York, 1965), pp. 406-411

14. "DSRV-1 Pressure Capsule Stress Analysis. Vol. III," LMSC Report D15446, Jan 1968, Ocean System Stress Group

15. Dyche, C., "User Instructions for PLOTOP, A Multiple-Option Plotting Subroutine in FORTRAN IV," LMSC B-70-67-38, Aug 1967

16. Bushnell, D., "Nonlinear Axisymmetric Analysis of Shells of Revolution," AIAA J., 5, pp. 432–439 (1967)

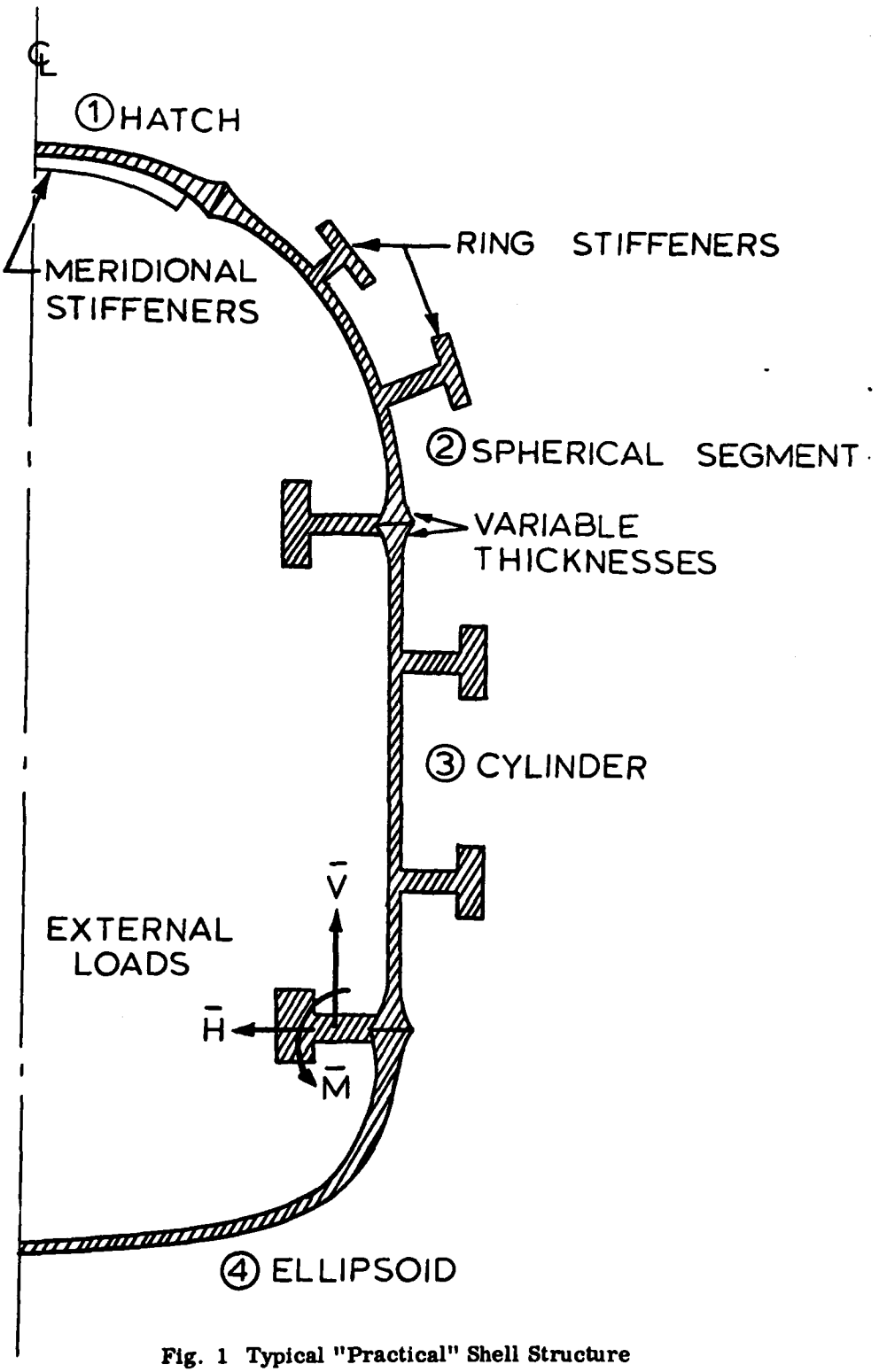

Fig. 1 Typical "Practical" Shell Structure

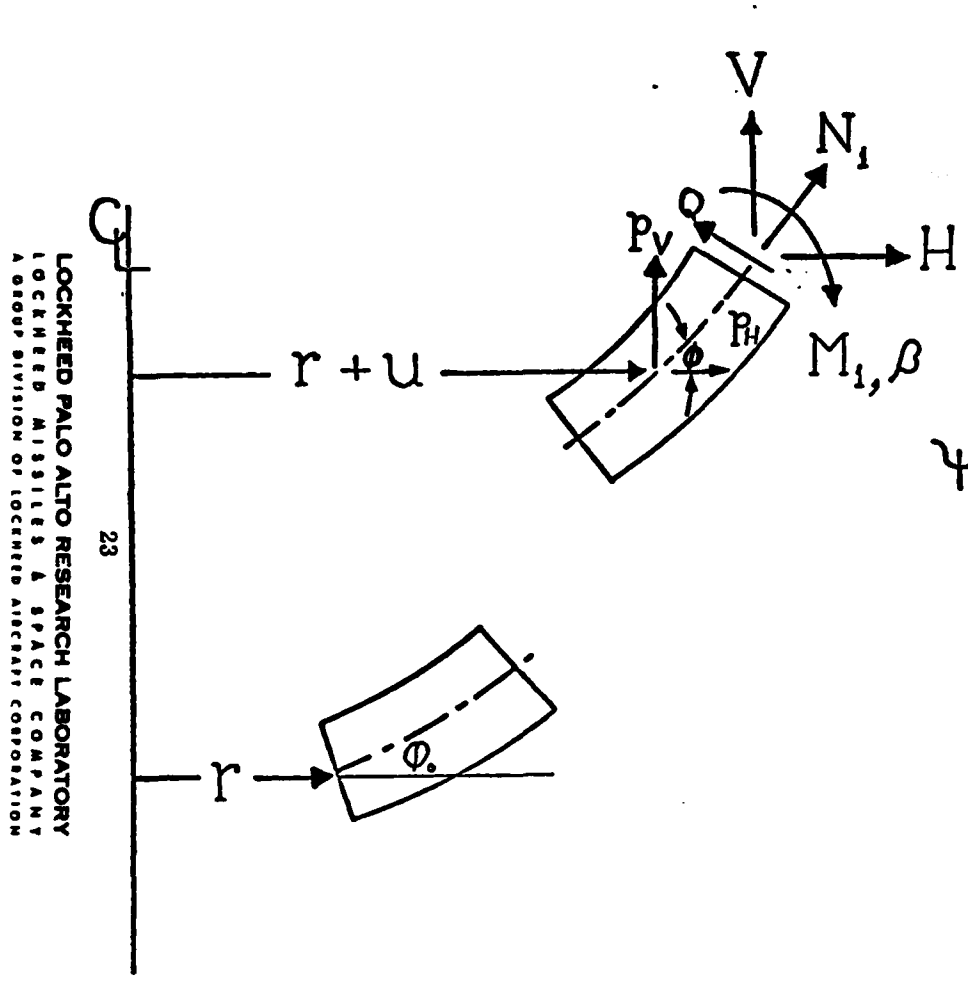

Fig. 2a Shell Elements

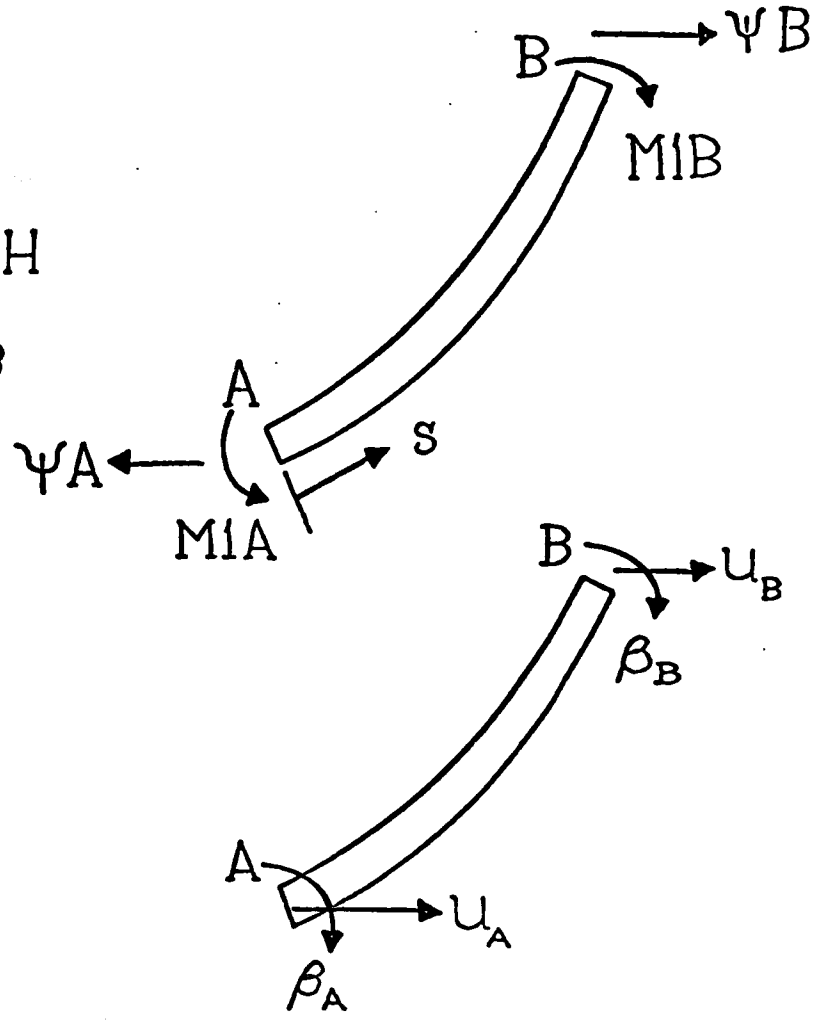

Fig. 2b Edge Forces and Displacements

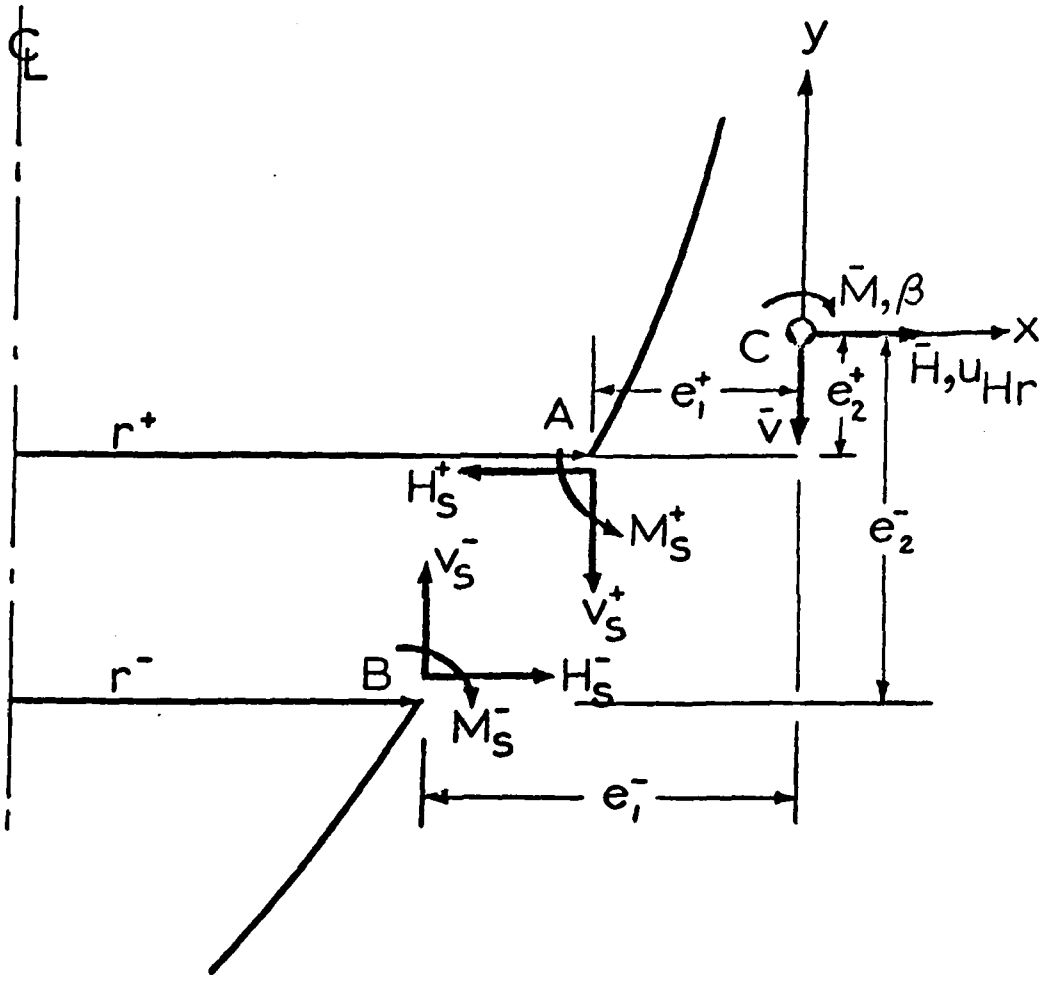

Fig. 3 Meridional Discontinuity With Ring Shear Center

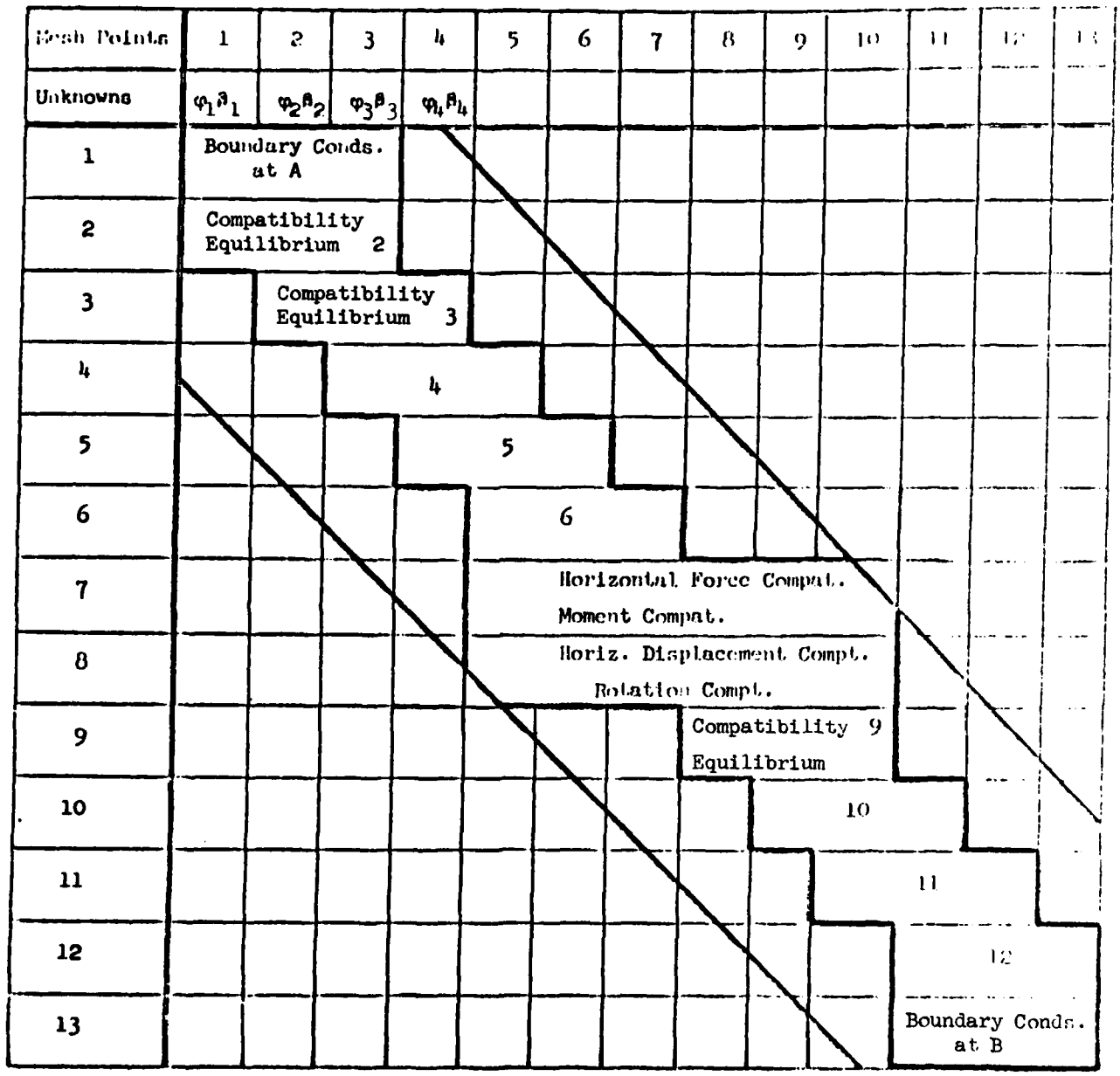

Fig. 4(a) Coefficient Matrix

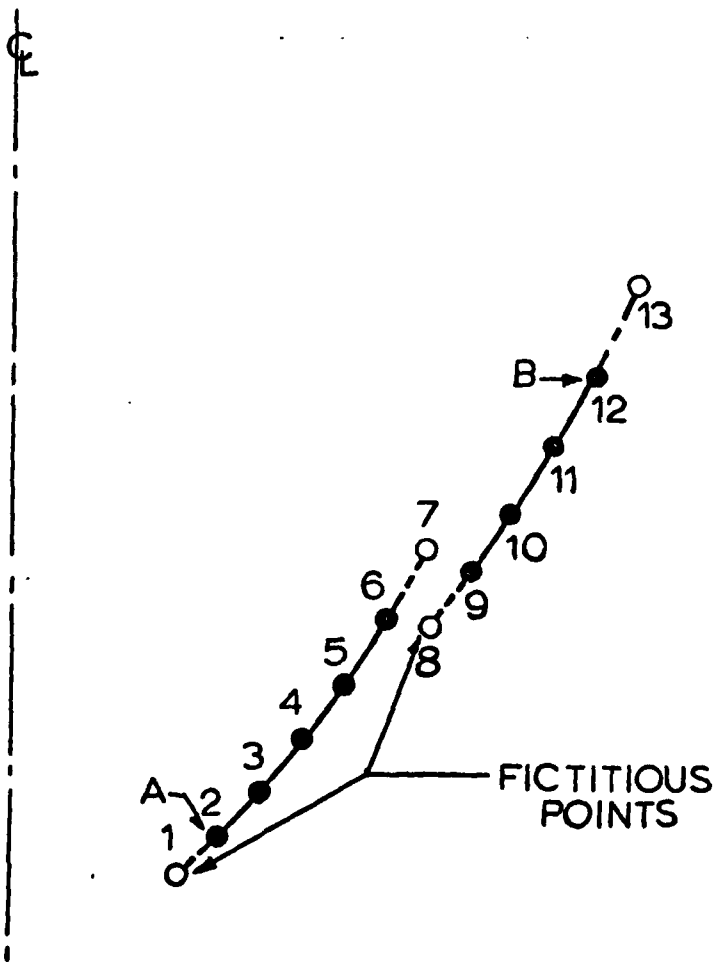

Fig. 4(b) Meridian with Mesh Points

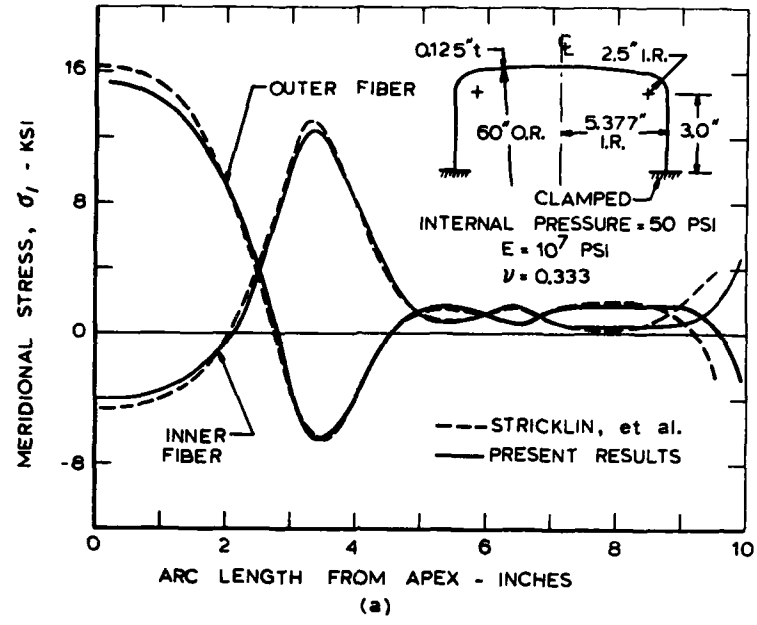

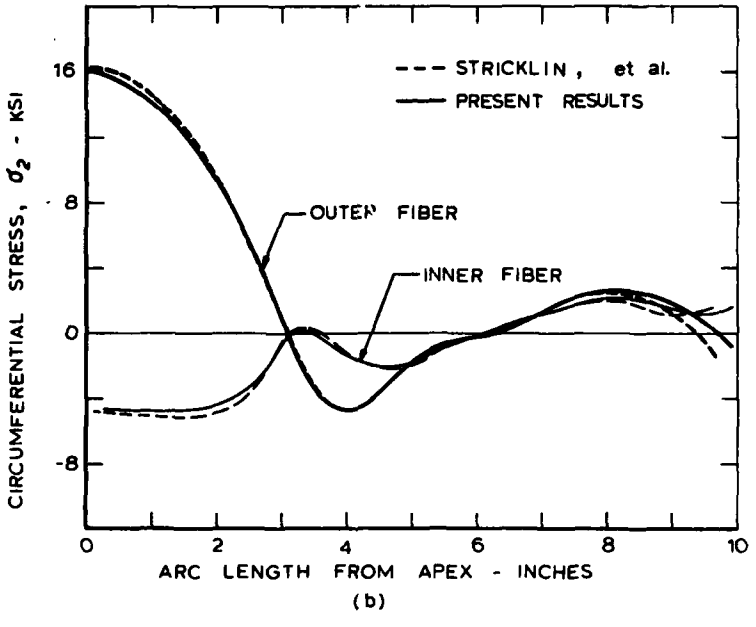

Fig. 5 Meridional and Circumferential Stresses in a Pressure Vessel With Internal Pressure. Comparison with the results of Ref. 12

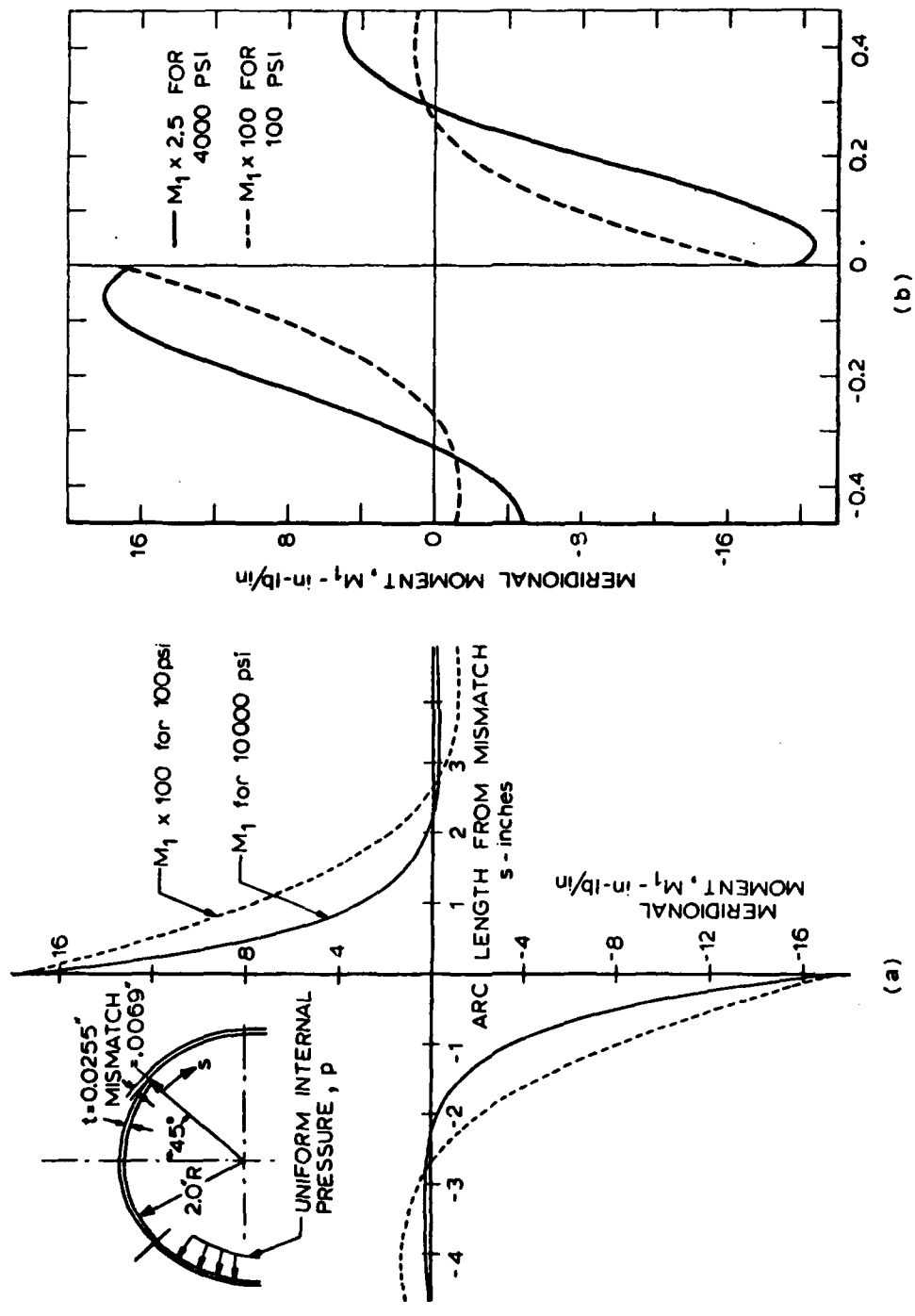

Fig. 6 Effect of (a) Internal and (b) External Pressure on the Discontinuity Bending Moment for a Sphere With a Mismatch

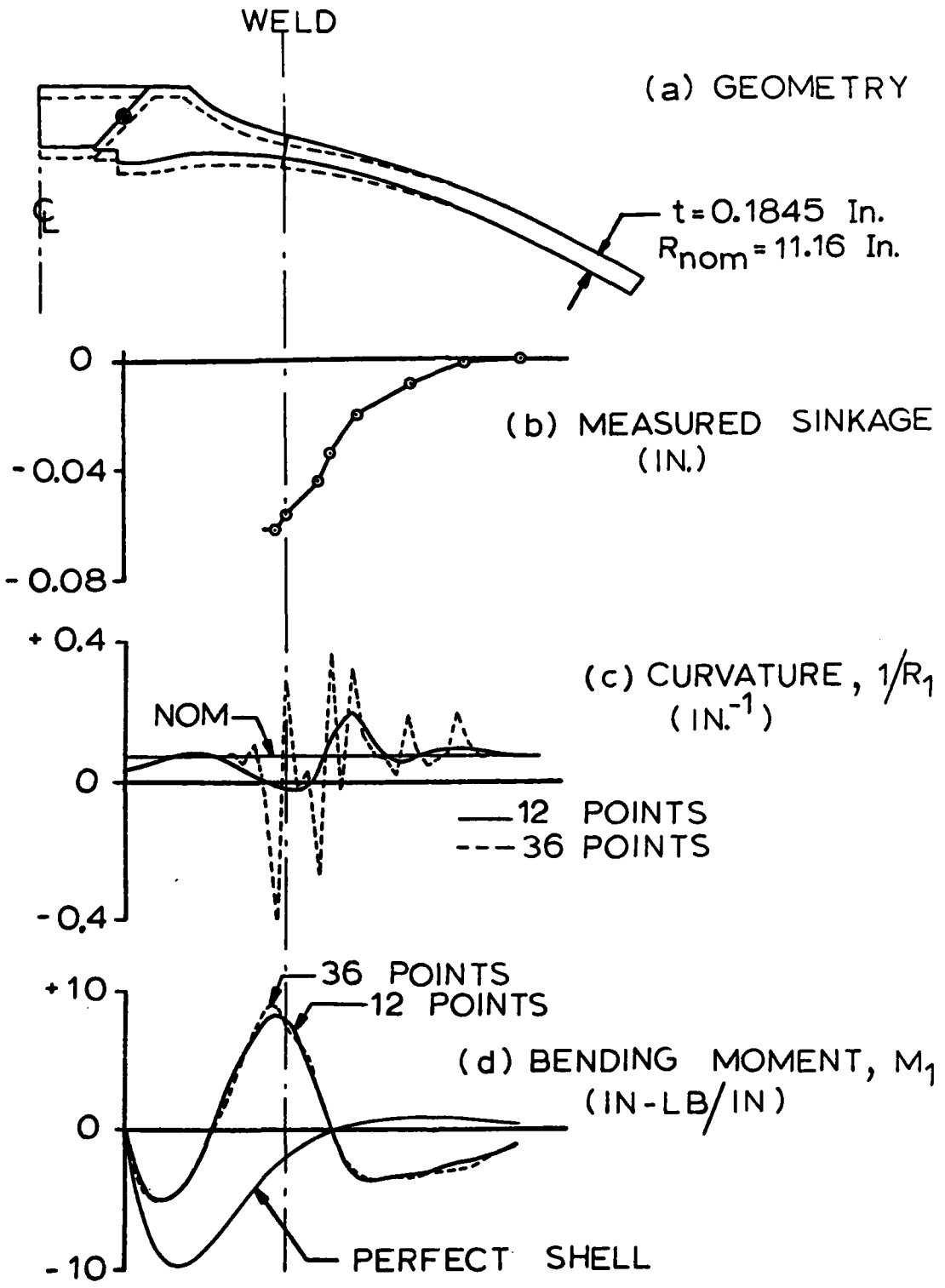

Fig. 7 Effect of Weld Sinkage on the Bending Moment Near a Viewport of a Pressure Hull

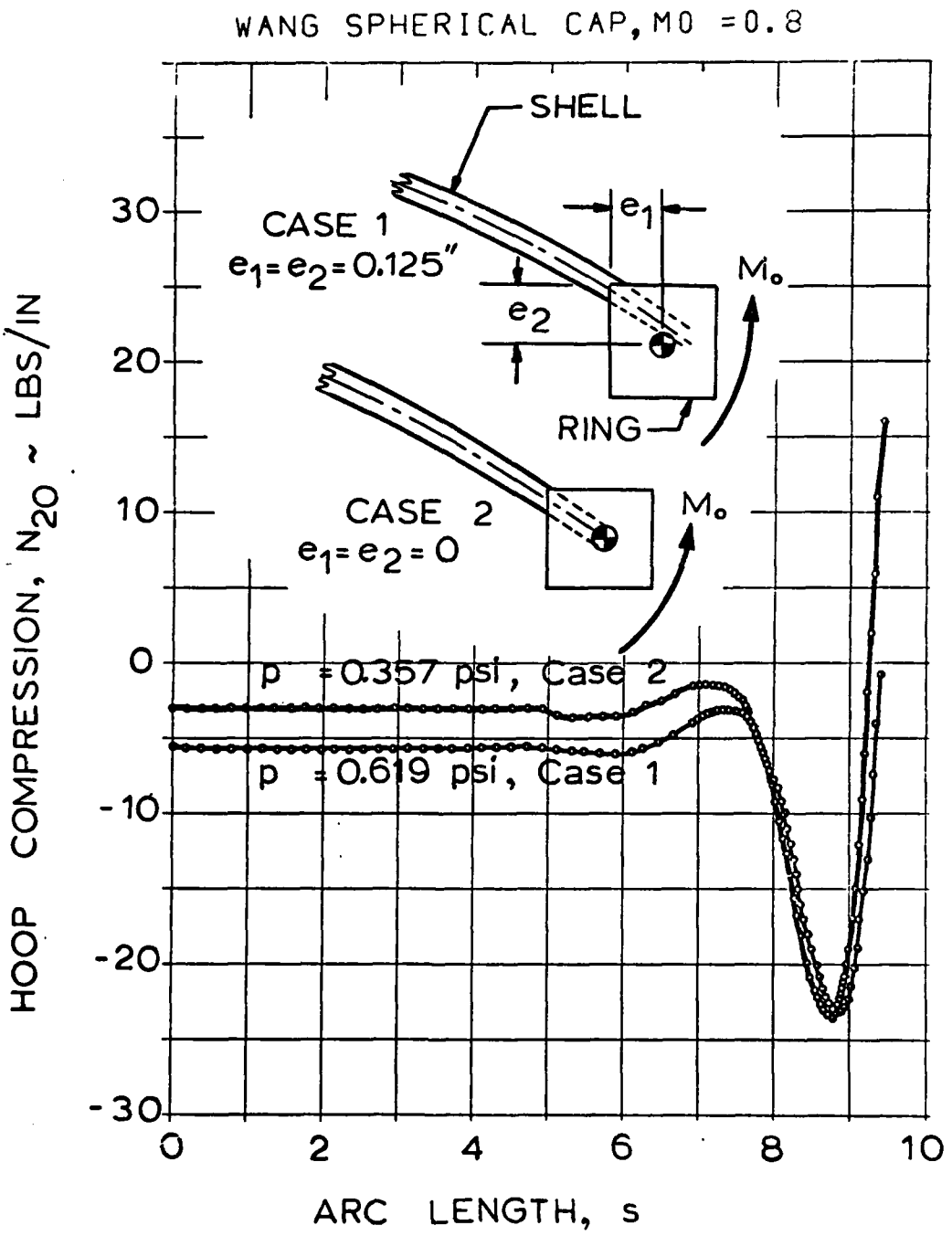

Fig. 8 Hoop Compression for Cases 1 and 2

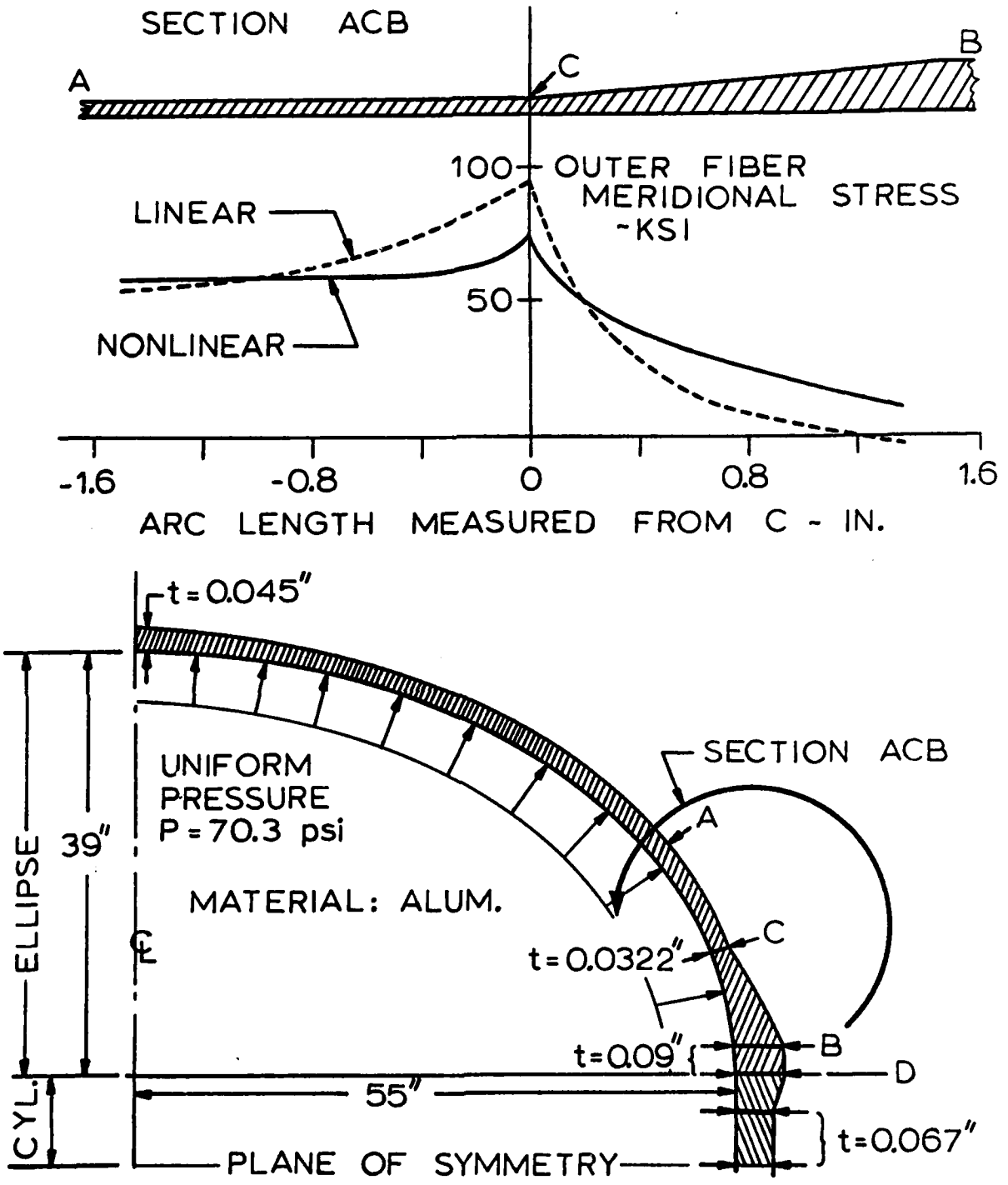

Fig. 9 Cryogenic Tank and Maximum Meridional Stress From Linear and Nonlinear Theories

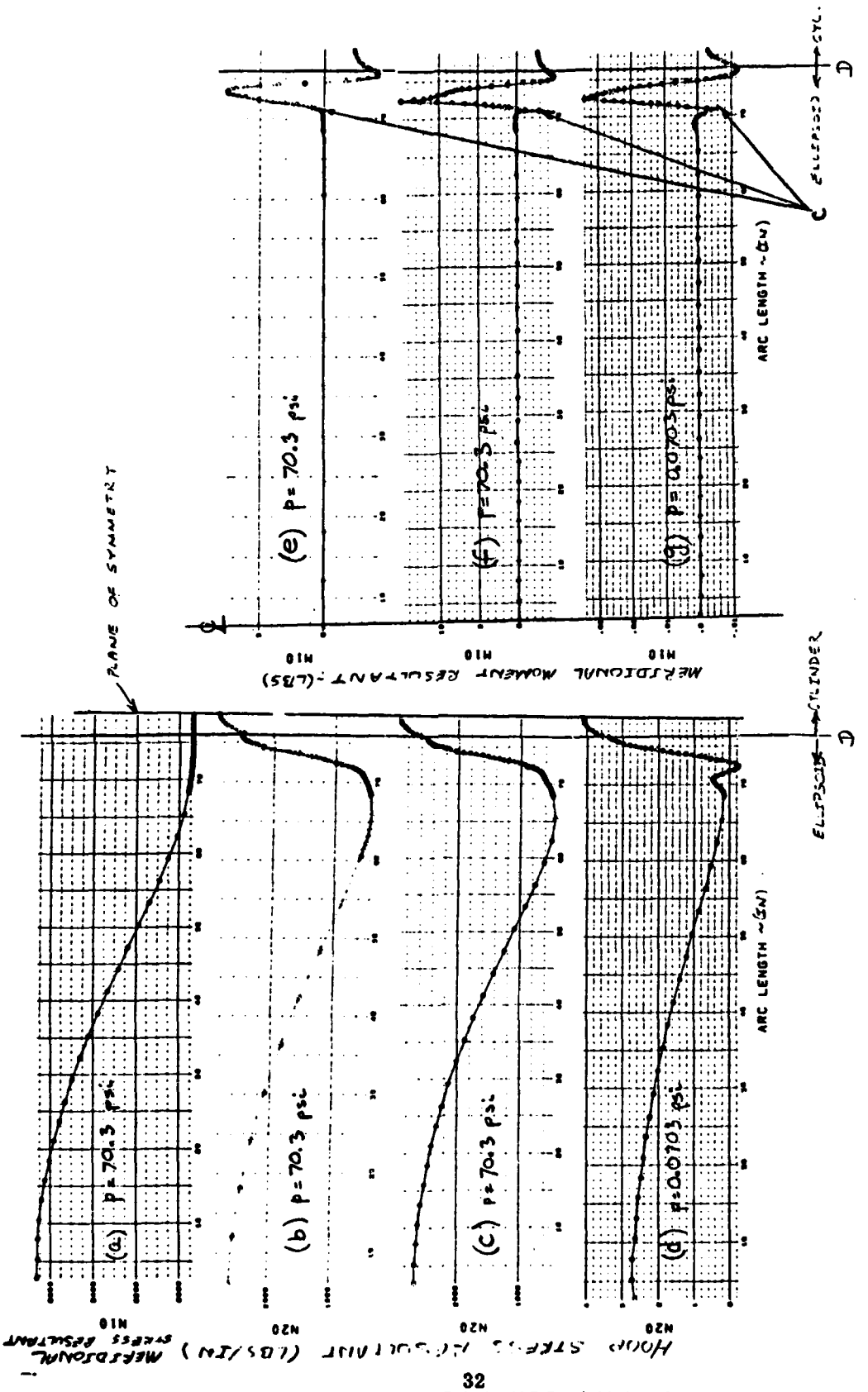

Fig. 10 Stress Resultants in Cryogenic Tank

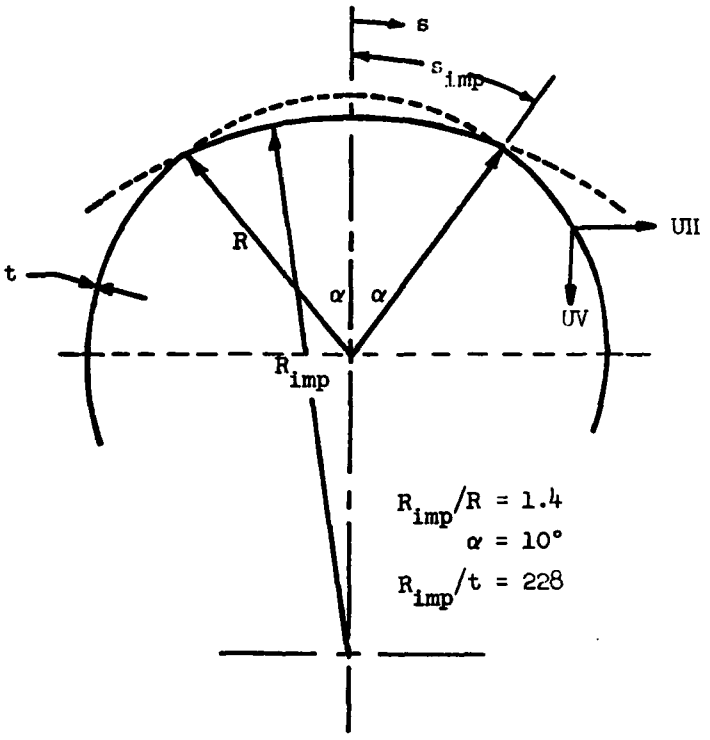

Fig. 11a Geometry of Spherical Shell With "Flat" Spot

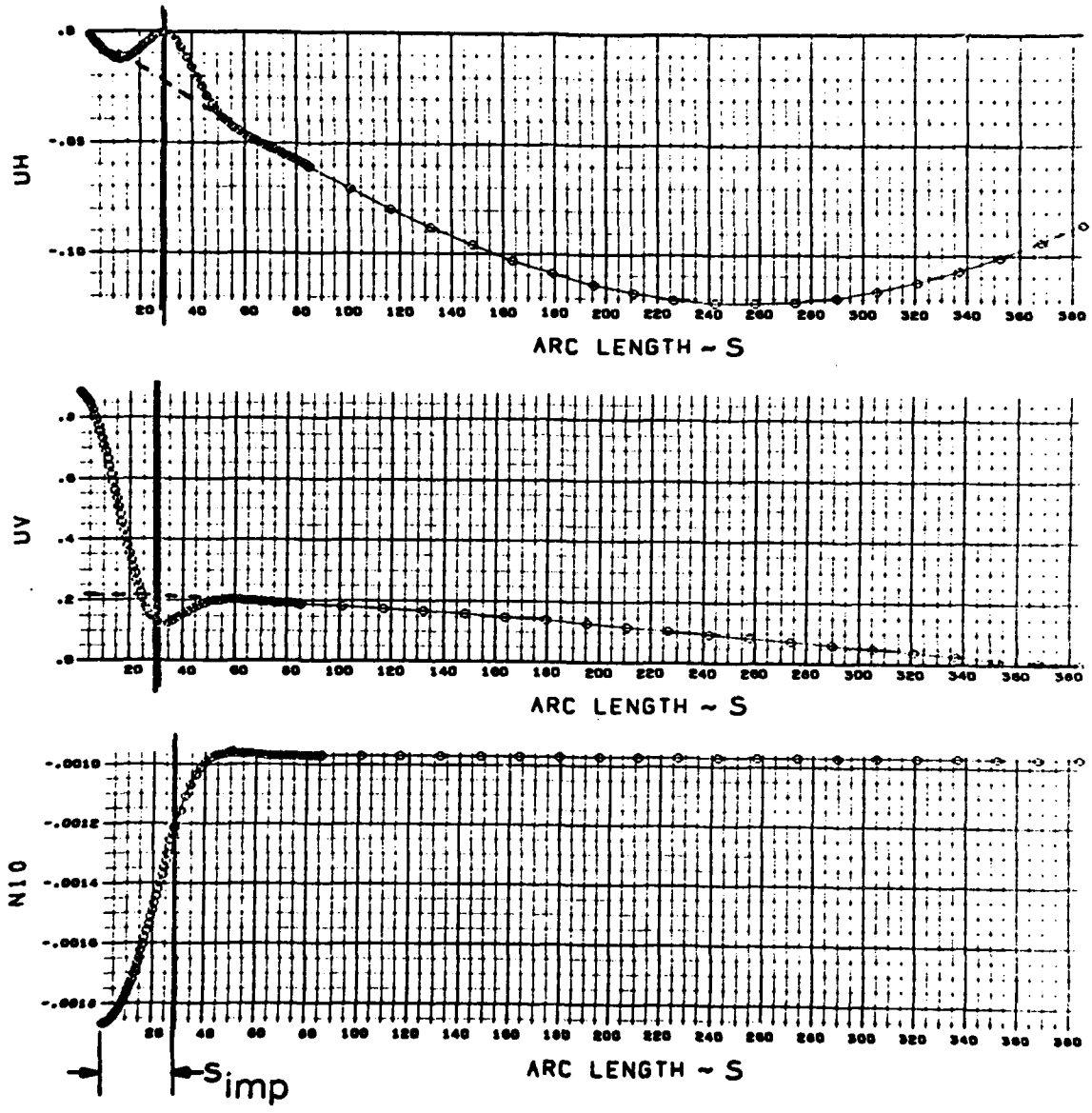

Fig. 11 Axisymmetric State of Shell With "Flat" Spot at Collapse
(b) Radial Displacement, Axial Displacement, and Meridional Stress Resultant

Lockheed Palo Alto Research Laboratory

Nonlinear Analysis for Axisymmetric Elastic Stresses in Ring-Stiffened, Segmented Shells of Revolution. Final Report on Contract N00014-67-C-0256. Palo Alto, Calif., September 1968.
35 p.

1. Shells of Revolution.
2. Nonlinear Analysis. I. N00014-67-C-0256.
II. LMSC N-26-68-2.

Lockheed Palo Alto Research Laboratory

Nonlinear Analysis for Axisymmetric Elastic Stresses in Ring-Stiffened, Segmented Shells of Revolution. Final Report on Contract N00014-67-C-0256. Palo Alto, Calif., September 1968.
35 p.

1. Shells of Revolution.
2. Nonlinear Analysis. I. N00014-67-C-0256.
II. LMSC N-26-68-2.

Lockheed Palo Alto Research Laboratory

Nonlinear Analysis for Axisymmetric Elastic Stresses in Ring-Stiffened, Segmented Shells of Revolution. Final Report on Contract N00014-67-C-0256. Palo Alto, Calif., September 1968.
35 p.

1. Shells of Revolution.
2. Nonlinear Analysis. I. N00014-67-C-0256.
II. LMSC N-26-68-2

Lockheed Palo Alto Research Laboratory

Nonlinear Analysis for Axisymmetric Elastic Stresses in Ring-Stiffened, Segmented Shells of Revolution. Final Report on Contract N00014-67-C-0256. Palo Alto, Calif., September 1968.
35 p.

1. Shells of Revolution.
2. Nonlinear Analysis. I. N00014-67-C-0256.
II. LMSC N-26-68-2

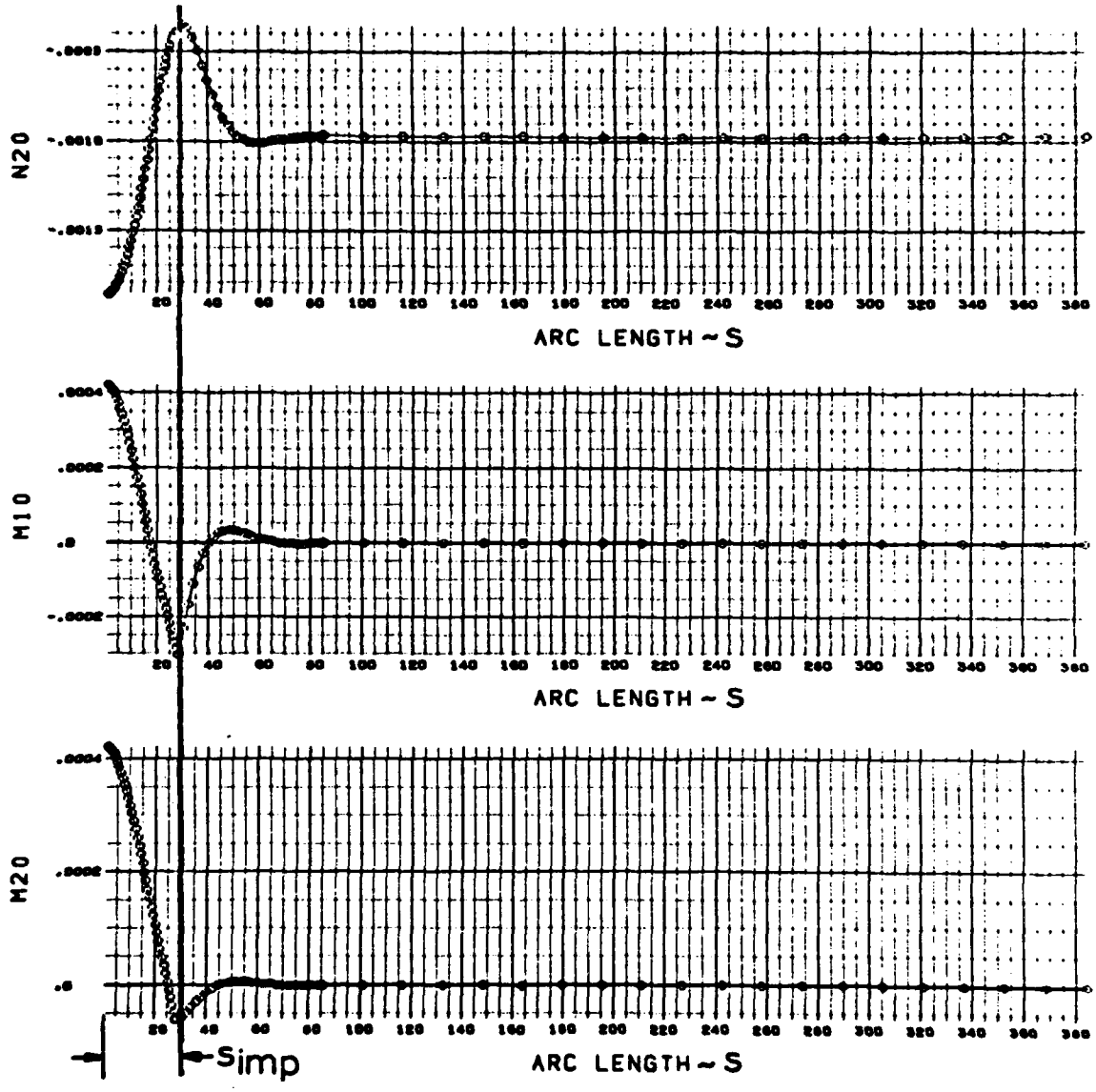

Fig. 11 Axisymmetric State of Shell With "Flat" Spot at Collapse
(c) Hoop Stress Resultant, Meridional Bending Moment, and Circumferential Bending Moment

UNCLASSIFIED

Security Classification

DOCUMENT CONTROL DATA - R & D

(Security classification of title, body of abstract and indexing annotation must be entered when the overall report is classified)

1. ORIGINATING ACTIVITY (Corporate author)	2a. REPORT SECURITY CLASSIFICATION
Lockheed Palo Alto Research Laboratory 3251 Hanover Street Palo Alto, California 94304	UNCLASSIFIED 2b. GROUP

3. REPORT TITLE

NONLINEAR ANALYSIS FOR AXISYMMETRIC ELASTIC STRESSES IN RING-STIFFENED, SEGMENTED SHELLS OF REVOLUTION

4. DESCRIPTIVE NOTES (Type of report and inclusive dates)

Final Report - June 1967 - September 1968

5. AUTHOR(S) (First name, middle initial, last name)

David (NMN) Bushnell

6. REPORT DATE	7a. TOTAL NO. OF PAGES	7b. NO. OF REFS
September 1968	35	15

8a. CONTRACT OR GRANT NO.	9a. ORIGINATOR'S REPORT NUMBER(S)
N00014-67-C-0256 b. PROJECT NO. SF 013 03 02 c. Task 1952 d.	N-26-68-2 9b. OTHER REPORT NO(S) (Any other numbers that may be assigned this report)

10. DISTRIBUTION STATEMENT

This document has been approved for public release and sale; its distribution is unlimited.

11. SUPPLEMENTARY NOTES	12. SPONSORING MILITARY ACTIVITY
	Naval Ship Research & Development Center Structural Mechanics Laboratory Washington, D. C. 20007

13. ABSTRACT

The finite-difference method is used for the nonlinear analysis of shells of revolution consisting of elastic shell segments of various geometries and wall constructions joined by elastic rings. The analysis and associated digital computer program were developed in response to the need for a better design tool for practical shell structures. Numerical results are presented for displacement and stress distributions in various pressure vessels. Particular emphasis is given to systems in which nonlinear effects are important and may influence the design. Values calculated with linear theory are compared with those from nonlinear theory.

DD FORM 1 NOV 65 1473

UNCLASSIFIED

Security Classification

14. KEY WORDS	LINK A		LINK B		LINK C	
	ROLE	WT	ROLE	WT	ROLE	WT
Stress Analysis, Shells of Revolution Computer Analysis of Shells Nonlinear Analysis Ring-Stiffened Shells						